Model Relaxations for the Fuel Cost Minimization of Steady–State Gas Pipeline Networks

Suming Wu
LIC Energy, Inc.
13831 Northwest Frwy., Suite 235
Houston, TX 77040
swu@licenergy.com

Roger Z. Ríos-Mercado
Texas A&M University
Department of Industrial Engineering
College Station, TX 77843
roger@habanero.tamu.edu

E. Andrew Boyd
PROS Strategic Solutions
3223 Smith St., Suite 100
Houston, TX 77006
boyd@prosx.com

L. Ridgway Scott
University of Chicago
Department of Computer Science
258 Ryerson Hall
Chicago, IL 60637
scott@uchicago.edu

January 1999

Abstract

Natural gas, driven by pressure, is transported through pipeline network systems. As the gas flows through the network, energy and pressure are lost due to both friction between the gas and the pipes' inner wall, and heat transfer between the gas and its environment. The lost energy of the gas is periodically restored at the compressor stations which are installed in the network. These compressor stations typically consume about 3–5% of the transported gas. This transportation cost is significant because the amount of gas being transported worldwide is huge. These facts make the problem of how to optimally operate the compressors driving the gas in a pipeline network important.

In this paper we address the problem of minimizing the fuel cost incurred by the compressor stations driving the gas in a transmission network under steady-state assumptions. In particular, the decision variables include pressure drops at each node of the network, mass flow rate at each pipeline leg, and the number of units to be operating within each compressor station. We present a mathematical model of this problem and an in-depth study of the underlying mathematical structure of the compressor stations. Then, based on this study, we propose two model relaxations (one in the compressor domain and another in the fuel cost function) and derive a lower bounding scheme. We also present empirical evidence that shows the effectiveness of the lower bounding scheme. For the small problems, where we were able to find optimal solutions, the proposed lower bound yields a relative optimality gap of around 15–20%. For a larger, more complex instance, it was not possible to find optimal solutions, but we were able to compute lower and upper bounds, finding a large relative gap between the two. We show this wide gap is mainly due to the presence of nonconvexity in the set of feasible solutions, since the proposed relaxations do a very good job of approximating the problem within each individual compressor station.

We emphasize that this is, to the best of our knowledge, the first time such a procedure (lower bound) has been proposed in over thirty years of research in the natural gas pipeline area.

Keywords: natural gas, pipelines, transmission networks, compressor stations, steady state, lower bounds, nonconvex objective

1 Introduction

Natural gas, driven by pressure, is transported through a pipeline network system. As the gas flows through the network, pressure (and energy) is lost due to both friction between the gas and the pipe inner wall, and heat transfer between the gas and its environment. To overcome this loss of energy and keep the gas moving, compressor stations are installed in the network, which consume part of the transported gas resulting in a fuel consumption cost. Principal concerns with both designing and operating a gas pipeline network are maximizing throughput and minimizing fuel cost. Numerical simulations based on either steady-state or transient models of the networks have been used to attempt to provide solutions to these problems. The problem we address in this paper is minimizing fuel cost for steady-state gas pipeline networks.

As the gas industry has developed, gas pipeline networks have evolved over decades into very large and complex systems. A typical network today might consist of thousands of pipes, dozens of stations, and many other devices, such as valves and regulators. Inside each station, there can be several groups of compressor units of various vintages that were installed as the capacity of the system expanded. Such a network may transport thousands of MMCFD (1 MMCFD = 10^6 cubic feet per day) of gas, of which 3–5% is used by the compressor stations to move the gas. It is estimated [12] that the global optimization of operations can save at least 20% of the fuel consumed by the stations. Hence, the problem of minimizing fuel cost is of tremendous importance.

With the aid of today's powerful digital computers, numerical simulation of gas pipeline networks can be very accurate. This opens the door to the development of optimization algorithms. Over the years many researchers have attempted this with varying degrees of success. The difficulties of such optimization problems come from several aspects. First, compressor stations are very sophisticated entities themselves. They might consist of a few dozen compressor units with different configurations and characteristics. Each unit could be turned on or off, and its behavior is nonlinear. Second, the set of constraints that define feasible operating conditions in the compressors along with the constraints in the pipes constitute a very complex system of nonlinear constraints. Surfing on such a manifold to attempt to find global optimal solutions demands an in-depth understanding of its structure. Finally, operations of the valves and regulators may introduce certain discontinuities to the problems as well.

The purpose of this paper is first to provide an in-depth study of the underlying mathematical structure of the compressor stations. Then, based on this study, we present a mathematical model of the fuel cost minimization problem, and derive a lower bounding scheme based on two model relaxations: (i) relaxation of the fuel cost objective function and (ii) relaxation of the non-convex nonlinear compressor domain. Finally, we present empirical evidence that shows the quality of the proposed relaxations.

The results are promising. For the small instances, where we were able to find both optimal solutions for the original problem (upper bound), and for the relaxed problem (lower bound) by an exhaustive approach, we found that the proposed relaxations yielded a relative optimality gap of around 15–20%. We also tested the procedure in a larger, more complex instance. For this instance, it was not possible to find optimal solutions, but it was still possible to calculate lower and upper bounds. We found that the proposed relaxations were in fact doing a good job of approximating the cost function within each individual compressor station. However, when optimizing over the complete domain (including all compressors at once, and other system constraints), the overall bound was not good due mainly to the non-convexity of the set of feasible solutions and to the presence of multiple local optima in the fuel cost function g.

We would like to emphasize that, to the best of our knowledge, this is the first time such a procedure (lower bound) has been proposed in over thirty years of research in the field of natural gas pipelines.

The rest of the paper is organized as follows. In Section 2 we highlight the most relevant work related to optimal operation on steady-state gas transmission networks. The compressor unit and station models we have developed are presented in Section 3. In Section 4, we formally introduce the fuel cost minimization problem and present several relaxations that allows us to devise a lower bounding scheme. These procedures have been tested with a few numerical examples in Section 5. We end the paper in Section 6 with our conclusions and directions for future work.

2 Related Work

Numerical simulations of gas pipeline networks have been carried out through this century and results can now be very accurate, especially with the aid of powerful digital computers. Osiadacz book [6] stands as the best reference on this subject.

The earlier work on developing optimization algorithms for fuel cost minimization in steady-state gas transmission networks can be traced back to Wong and Larson's work [13] in 1968, which made use of dynamic programming (DP) techniques to solve problems with simple "gun-barrel" network structures. More recently, Lall and Percell [3] present a DP algorithm that handles topologies with diverging branches, and incorporates into the model decision variables for representing the number of units to be operated within each compressor station. More recently, Carter [2] develops a non-sequential DP algorithm to handle looped networks when the mass flow rate variables are fixed. The main advantages of DP are that a global optimum is guaranteed to be found and that nonlinearity can be easily handled. Disadvantages of DP are that its application is practically limited to the networks with simple structures, such as "gun-barrel" or tree topologies, and that computation increases exponentially in the dimension of the

problem, commonly referred as *the curse of dimensionality.* Percell and Ryan [10] addressed the problem by using the generalized reduced gradient (GRG) for nonlinear optimization. Advantages of the GRG method are that it avoids the dimensionality problem and that it may be applied to networks with loops. However, since the GRG method was based on a gradient search method, it is not theoretically guaranteed to find a global optimum, especially in the presence of discrete decision variables, and it may stall at local minima.

In [15], Wu et al. present a mathematical model for the fuel cost minimization over a single unit compressor station. Some of the properties studied in that paper have been extended here to handle stations with multiple compressor units.

Optimization techniques have also been applied for transient (time dependent) models (e.g., Osiadacz [7], and Osiadacz and Swierczewski [9]), and network design (e.g., Osiadacz and Górecki [8]), with modest success. It is important to mention that optimization approaches developed to date work well under some general assumptions; however, as the problems become more complex, the need arises for further research and effective development of algorithms from the optimization perspective.

3 Compressor Units and Stations

In general, compressor stations in gas pipeline networks can be very complicated because they may consist of up to dozens of compressor units of different types with various configurations. Two main types of compressor units used in today's gas industry are centrifugal and reciprocating compressor units. In this paper we consider only those compressor stations which consist of several identical centrifugal compressor units in parallel. This type of station is very common in today's gas industry, and having an understanding of this type of station is fundamental for modeling more complex station configurations.

3.1 Single Centrifugal Compressor Units

The primal quantities related to a centrifugal compressor unit are inlet volumetric flow rate Q, speed S, adiabatic head H, and adiabatic efficiency η. It has been recognized [10] that the relationship among these quantities can be well described by the following two equations:

$$H/S^2 = A_H + B_H(Q/S) + C_H(Q/S)^2 + D_H(Q/S)^3, \tag{1}$$

$$\eta = A_E + B_E(Q/S) + C_E(Q/S)^2 + D_E(Q/S)^3, \tag{2}$$

where A_H, B_H, C_H, D_H, A_E, B_E, C_E, and D_E are constants which depend on the compressor unit and are typically estimated by applying the least squares method to a set of collected data of the quantities Q, S, H, and η. Four other parameters are usually provided. They are

minimum speed $S_{\min}$, maximum speed $S_{\max}$, surge limit $surge$, and stonewall limit $stonewall$. These give the limits to the speed S and the ratio of Q to S, i.e.,

$$S_{\min} \leq S \leq S_{\max}, \tag{3}$$

$$surge \leq Q/S \leq stonewall. \tag{4}$$

Figures 1 and 2 show the set of data collected from a typical centrifugal unit. In Figure 1, we plot H vs. Q, showing the control lines for S (between $S_{\min}$ and $S_{\max}$) and Q/S (between $surge$ and $stonewall$), generated by equation (1). A plot of equation (2) is illustrated in Figure 2.

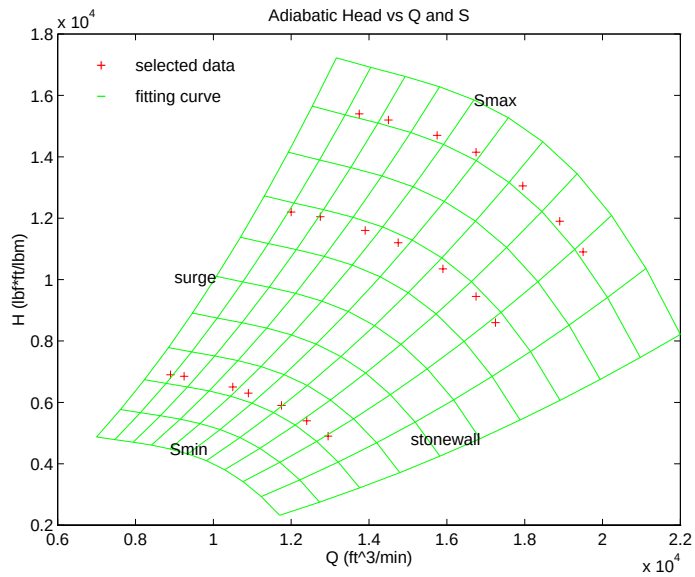

Figure 1: Operation envelope in Q, S, and H (single centrifugal unit)

3.1.1 Feasible Domain for a Single Unit

The inequalities (3) and (4) together with equation (1) actually constitute a feasible operating domain for the unit. Figure 1 shows the feasible domain in terms of Q, S, and H. Since, the preferred variables from the network modeling perspective are mass flow rates and pressures, we proceed to map the above operation envelope into a three-dimensional domain, denoted as D^{unit}, consisting of the following variables: mass flow rate v, suction pressure p_s, and discharge pressure p_d. The relationships between (H, Q) and (v, p_s, p_d) are the following:

$$H = \frac{ZRT_s}{m}\left[\left(\frac{p_d}{p_s}\right)^m - 1\right], \tag{5}$$

and

$$Q = ZRT_s\frac{v}{p_s}, \tag{6}$$

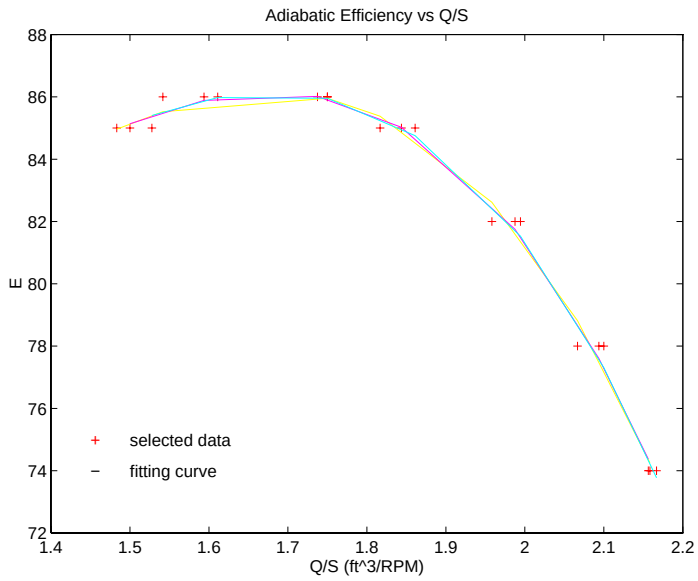

Figure 2: Adiabatic efficiency as a function of Q/S

where $m = \frac{k-1}{k}$, the specific heat ratio k, the gas compressibility factor (or Z-factor) Z, and the gas constant R, are positive parameters. The suction temperature T_s will be assumed to be constant in this work.

By (3) and (4), it follows that the inlet volumetric flow rate Q must satisfy

$$Q^L \leq Q \leq Q^U, \tag{7}$$

where $Q^L = S_{\min} * surge$ and $Q^U = S_{\max} * stonewall$. For each Q within this range, the adiabatic head H is bounded below by either $S_{\min}$ or *stonewall* and bounded above by either $S_{\max}$ or *surge*, see Figure 1. Let $H^L(Q)$ and $H^U(Q)$ be the lower and upper bound functions in Figure 1, respectively. Then

$$H^L(Q) \leq H \leq H^U(Q), \quad Q^L \leq Q \leq Q^U.$$

Besides, the unit should have pressure limits, say p_s^L and p_s^U for suction pressure p_s. Hence, the feasible domain D^{unit} for a single centrifugal unit is

$$D^{\text{unit}} = \left\{ (v, p_s, p_d) : \; p_s^L \leq p_s \leq p_s^U, \; V^L \leq \frac{v}{p_s} \leq V^U, \; G^L\left(\frac{v}{p_s}\right) \leq \frac{p_d}{p_s} \leq G^U\left(\frac{v}{p_s}\right) \right\}, \tag{8}$$

where

$$V^L = \frac{Q^L}{ZRT_s}, \tag{9}$$

$$V^U = \frac{Q^U}{ZRT_s}, \tag{10}$$

$$G^L(q) = \left[1 + \frac{m}{ZRT_s} H^L(ZRT_s q)\right]^{\frac{1}{m}}, \tag{11}$$

$$G^U(q) \quad = \quad \left[1 + \frac{m}{ZRT_s} H^U(ZRT_s q)\right]^{\frac{1}{m}}. \tag{12}$$

Figure 3 shows the entire domain D^{unit}, where the shadowed band in the middle corresponds to the domain's profile for p_s fixed. This two-dimensional profile can be seen in Figure 4.

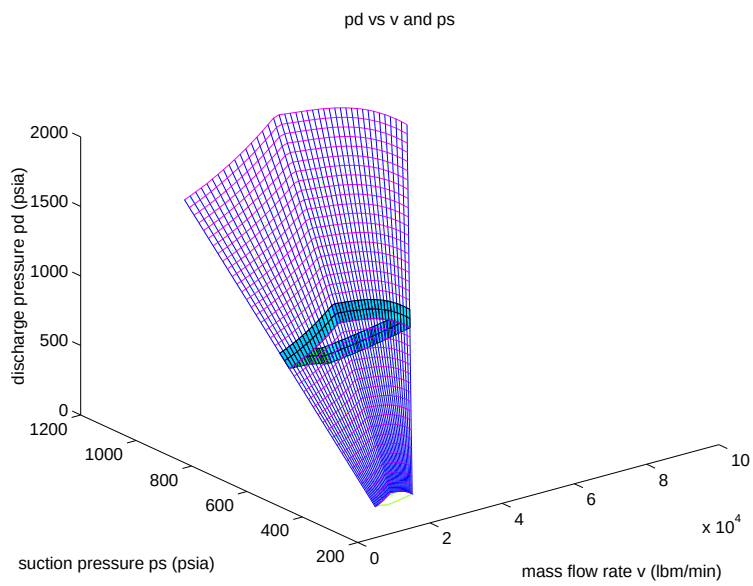

Figure 3: Feasible domain D^{unit} for a single compressor unit

Let us point out a few properties of the domain D^{unit}. First of all, by its definition (8), the domain D^{unit} is bounded. The upper surface bounding the domain D^{unit} is

$$\left\{(v(t,x), p_s(t,x), p_d(t,x)) = \left(t\,x, t, G^U(x)\,t\right) : \; p_s^L \le t \le p_s^U, \; V^L \le x \le V^U\right\}. \tag{13}$$

When x is fixed, the above surface gives a straight line segment, i.e.,

$$\left\{(v(t), p_s(t), p_d(t)) = \left(t\,x, t, G^U(x)\,t\right) : \; p_s^L \le t \le p_s^U\right\}. \tag{14}$$

Notice that, for all x, we get $(v(0), p_s(0), p_d(0)) = (0,0,0)$; that is, all these lines pass through the origin. The same is true for the lower bounding surface.

Second, as shown in Figure 4, D^{unit} is not a convex set. Note that arcs AD and BC are convex, while DB and AC are concave. This non-convexity property is common for centrifugal compressor units.

3.1.2 Fuel Cost Function for a Single Unit

Basically, we will be working in the (v, p_s, p_d) space. To find out how to run the compressor station so as to achieve a given feasible value (v, p_s, p_d), we proceed to map that point back to the original operating space by first computing H and Q from equations (5) and (6), respectively, and then solving for S in (1).

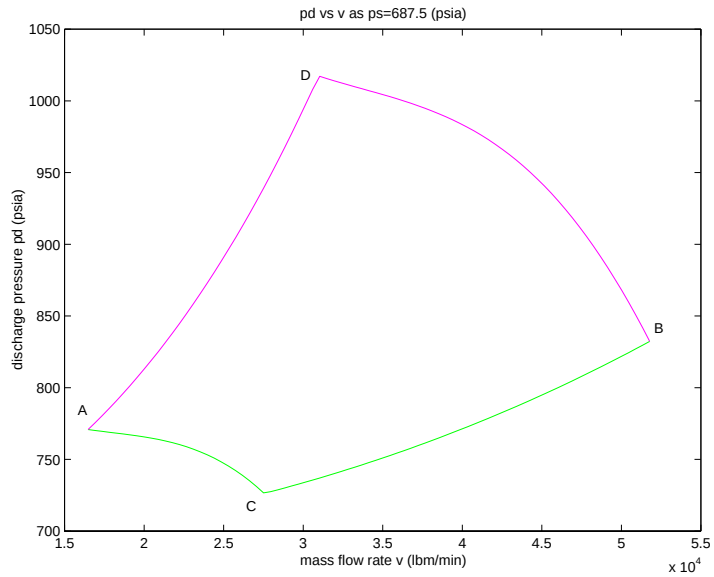

Figure 4: Profile of domain D^{unit} for p_s fixed

The fuel cost g^{unit} is given by

$$g^{\text{unit}}(v,\, p_s,\, p_d) = \alpha \frac{vH}{\eta}, \quad \forall (v,\, p_s,\, p_d) \in D^{\text{unit}}, \tag{15}$$

where α is a positive constant, which, for simplicity, is assumed to be equal to 1 throughout this work. Hence, function $g^{\text{unit}}(v,\, p_s,\, p_d)$ is implicitly defined, with equations (5), (6), (1), and (2), on domain D^{unit}. Each evaluation of $g^{\text{unit}}(v,\, p_s,\, p_d)$ has to solve the nonlinear equations (1)-(2). The behavior of the function $g^{\text{unit}}(v,\, p_s,\, p_d)$, of course, depends on the characteristics of the compressor unit. However, it is typical that the fuel cost g^{unit} increases with respect to both the compressor ratio p_d/p_s and the volumetric flow rate Q, or v/p_s, and decreases with respect to the suction pressure p_s. The surface of function $g^{\text{unit}}(v,\, p_s,\, p_d)$ when p_s is fixed is plotted in Figure 5.

3.1.3 Approximations of the Fuel Cost Function

As we have seen above, each evaluation of function $g^{\text{unit}}(v,\, p_s,\, p_d)$ involves solving a nonlinear equation (1)–(2). This is not a desirable property by any means since most of the optimization techniques require many function evaluations within their algorithmic framework. On the other hand, the function g^{unit}, as shown in Figure 5, is smooth and has some monotonicity properties. Hence, many researchers have suggested a simple function approximation of g^{unit}. The most frequently used functions are polynomials of variables $(v,\, p_s,\, p_d)$ of degree 1 or 2, i.e.,

$$g_1(v,\, p_s,\, p_d) = A_1 v + B_1 p_s + C_1 p_d + D_1, \tag{16a}$$

$$g_2(v,\, p_s,\, p_d) = A_2 v^2 + B_2 v p_s + C_2 v p_d + D_2 p_s^2 + E_2 p_s p_d \tag{16b}$$

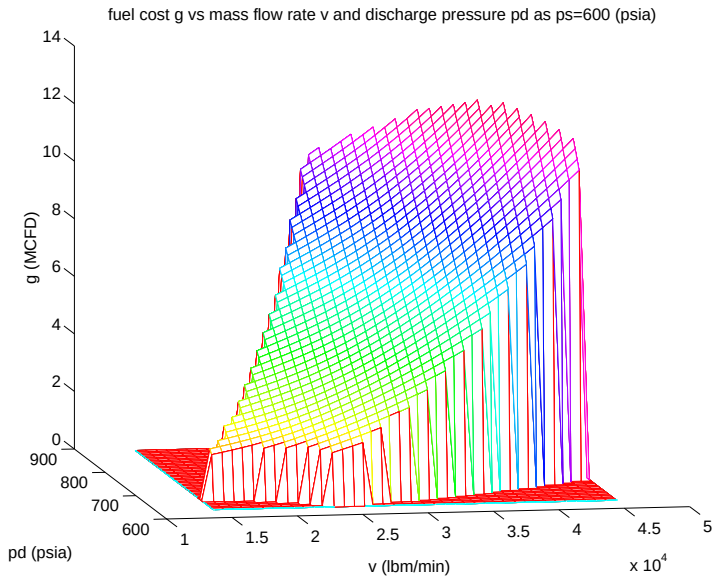

Figure 5: Fuel cost function $g^{\text{unit}}(v, p_s, p_d)$ for p_s fixed

$$+ F_2 p_d^2 + G_2 v + H_2 p_s + I_2 p_d + J_2.$$

To look for functions in categories other than polynomials of variables $(v,\ p_s,\ p_d)$, we first notice that, since g can also be seen as a function of v/p_s and p_d/p_s, it might be advantageous to use the following functions to approximate the function g^{unit}:

$$g_3(v,\ p_s,\ p_d) = p_s \left(A_3 \frac{v}{p_s} + B_3 \frac{p_d}{p_s} + C_3 \right) \tag{16c}$$

$$g_4(v,\ p_s,\ p_d) = p_s \left(A_4 \left(\frac{v}{p_s}\right)^2 + B_4 \frac{v}{p_s}\frac{p_d}{p_s} + C_4 \left(\frac{p_d}{p_s}\right)^2 + D_4 \frac{v}{p_s} + E_4 \frac{p_d}{p_s} + F_4 \right) \tag{16d}$$

$$g_5(v,\ p_s,\ p_d) = v \left(A_5 \frac{v}{p_s} + B_5 \frac{p_d}{p_s} + C_5 \right) \tag{16e}$$

$$g_6(v,\ p_s,\ p_d) = v \left(A_6 \left(\frac{v}{p_s}\right)^2 + B_6 \left(\frac{p_d}{p_s}\right)^2 + C_6 \frac{v}{p_s}\frac{p_d}{p_s} + D_6 \frac{v}{p_s} + E_6 \frac{p_d}{p_s} + F_6 \right) \tag{16f}$$

In preliminary testing we have compared each of these approximation functions to the fuel cost function g^{unit}. The maximum relative approximation errors for the unit shown in Figures 1 and 2 with p_s ranging between 60–800 (psia) are displayed in Table 1.

As can be seen, function g_6 fits the fuel cost function g^{unit} very well. Function g_4 is also good. Function g_5 is good as it takes a more simple form than g_6 and g_4. We also observed that g_2 fits the g^{unit} much better than g_5 in most of the domain D^{unit}, and within these part it can be as good as g_6. The large maximum relative error of g_2 is due to its bad behavior in a very small part of the domain, typically near the boundary. For the rest of our study, we use function g_6 as an approximation to the cost function g^{unit}.

Function	Maximum relative error (%)
g_1	66.15
g_2	57.60
g_3	66.15
g_4	5.85
g_5	10.06
g_6	2.67

Table 1: Evaluation of approximation functions

3.2 Compressor Stations with Identical Parallel Units

3.2.1 Feasible Domain for a Station

Now, let us consider a compressor station with N parallel identical units. Let (v, p_s, p_d) be the mass flow rate, suction pressure, and discharge pressure for the station, respectively. We assume here the suction and discharge pressures of the station are the same as those of the individual units in the station. However, the mass flow rate v through the station will be equally divided to pass through the units which are selected to run. Hence, if only one unit is selected to run, then the feasible domain, denoted as D^1, is the same as the feasible domain D^{unit} for a single unit which is represented in (8). When r units are selected to run, $1 \leq r \leq N$, then the feasible domain, denoted by D^r is

$$D^r = \left\{ (v, p_s, p_d) : \ (v/r, p_s, p_d) \in D^1 \right\}. \tag{17}$$

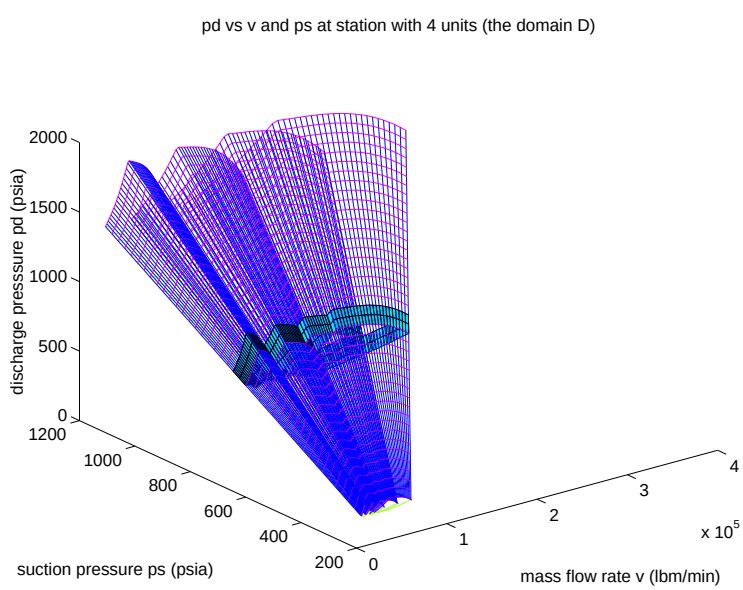

Figure 6: Feasible domain D for a station with 4 parallel units

Suppose that at least one unit in the station must be run; the whole feasible domain D of the station is thus the union of D^r

$$D = \bigcup_{r=1}^{N} D^r. \tag{18}$$

The domain D of a station with 4 identical units is shown in Figure 6, where the shadowed area in the middle represents its profile when p_s is fixed. This profile is shown in Figure 7.

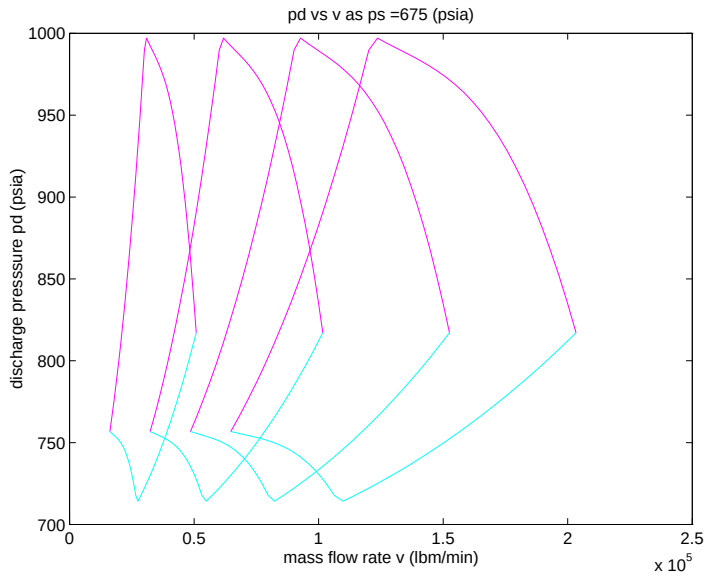

Figure 7: Profile of domain D for a station with 4 parallel units

Although it depends on the characteristics of the units installed in the station, as we have seen, the domain D of the station shown in the above figures is connected. Here we shall give a necessary condition for D to be connected.

Lemma 1 *If the feasible domain D of a station with identical parallel units is connected, then*

$$\frac{Q^U}{Q^L} \geq 2,$$

where Q^L and Q^U are the minimum and maximum volumetric flow rate of the units, respectively.

Proof: We first note that, by the definition (8), $D^1 = D^{\text{unit}}$ is connected. For any $r: \ 1 \leq r \leq N$, by (17), D^r is an affine image of D^1; thus, D^r is connected.

Suppose that D is connected. By (18), there is an $r > 1$, such that $D^1 \cap D^r$ is nonempty. Hence, there exists a triple value $(v, p_s, p_d) \in D^1 \cap D^r$. By (8), we get

$$V^L \leq \frac{v}{p_s} \leq V^U, \quad V^L \leq \frac{v}{rp_s} \leq V^U.$$

Thus, $rV^L \leq \frac{v}{p_s} \leq V^U$, i.e.,

$$r \leq \frac{V^U}{V^L}.$$

Since $r > 1$ and $V^U/V^L = Q^U/Q^L$, we get

$$\frac{Q^U}{Q^L} \geq 2,$$

and the proof is complete. ■

It can be seen from these figures that domain D^r is obtained by extending domain D^1 r times in the direction of v. Hence, it has the same properties as D^{unit} does.

3.2.2 Minimum Fuel Cost Function for a Station

For some values $(v, p_s, p_d) \in D$, Figure 7 clearly indicates that one may achieve them by selecting a different number of units to run. However, fuel costs could be different among these selections. This is because changing the number of running units changes the inlet volumetric flow rate, and so changes the adiabatic efficiency for each running unit. Figure 8 shows the fuel costs for a 4-unit station obtained by running 1, 2, 3, or 4 units separately.

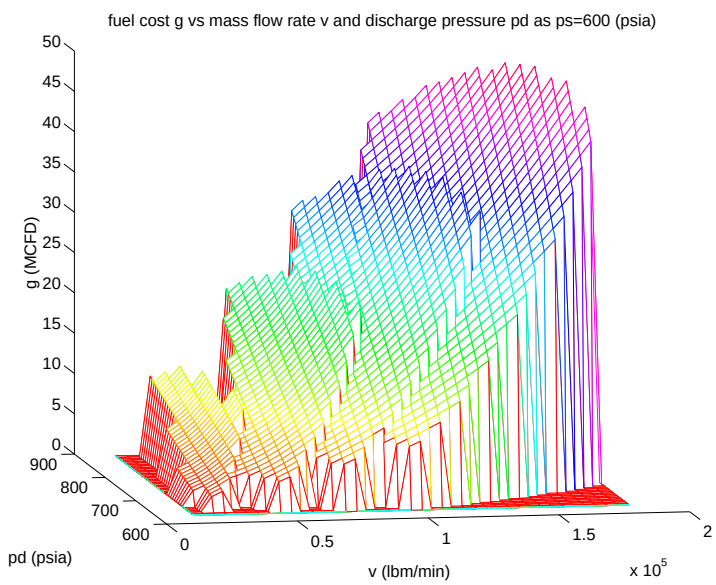

Figure 8: Fuel cost by running different numbers of units for a station with 4 parallel units

Let $\mathcal{R}$ be the set of feasible values of r for a given $(v, p_s, p_d) \in D$, i.e.,

$$\mathcal{R} \quad = \quad \{r : r \text{ is integer }, 1 \leq r \leq N, (v, p_s, p_d) \in D^r\}.$$

The following result on $\mathcal{R}$ can be easily verified.

Proposition 1 *For any $(v, p_s, p_d) \in D$, if $r_1, r_2 \in \mathcal{R}$, then, for any integer r with $r_1 \leq r \leq r_2$, we have $r \in \mathcal{R}_{(v,p_s,p_d)}$.*

The above proposition implies that, for any $(v, p_s, p_d) \in D$, the set $\mathcal{R}$ is an interval of integers. When the station variables are given as $(v, p_s, p_d) \in D$, and the number of units selected to run is $r \in \mathcal{R}$, the suction and discharge pressures for each running unit are p_s and p_d, respectively, while the mass flow rate through each unit is v/r. Hence, the fuel consumed by each running unit is equally $g^{\text{unit}}(v/r, p_s, p_d)$. Since r units have been selected to run in the station, the total fuel consumed by the station is $rg^{\text{unit}}(v/r, p_s, p_d)$. The minimum fuel cost is thus

$$g(v, p_s, p_d) = \min_{r \in \mathcal{R}} \left\{ rg^{\text{unit}}(v/r, p_s, p_d) \right\}, \tag{19}$$

where $g^{\text{unit}}(v/r, p_s, p_d)$ is given by (15). Hence, the value of the minimum fuel cost function $g(v, p_s, p_d)$ is the solution of the above integer program with a single integer variable r. Figure 9 plots the function g as p_s is fixed for a 4-unit station.

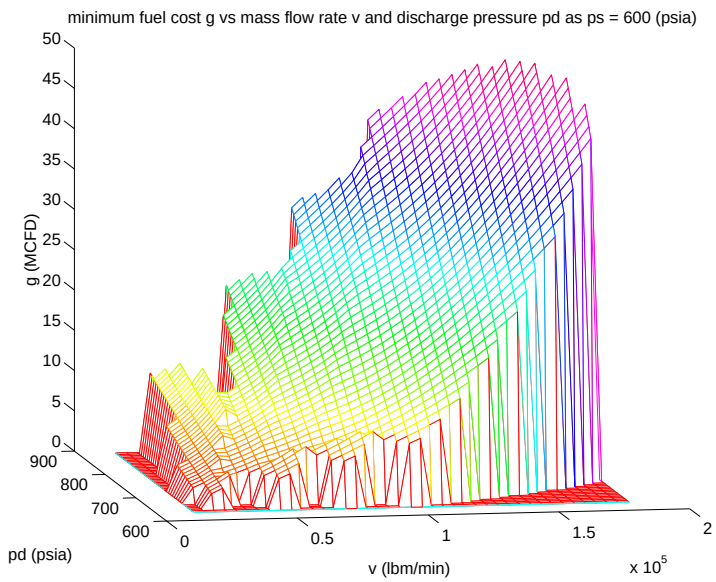

Figure 9: Minimum fuel cost as a function of v and p_d for a station with 4 parallel units

The surface of the minimum fuel cost function g may or may not have jumps. It depends on the characteristics of the units in the station. In this example, it is mostly continuous except at the boundary of D^2 which is in D^1. Compare Figure 9, which shows the minimum fuel cost function, with Figure 8, which shows the fuel cost for different values of r.

As we have shown in this section, the domain D of the station is non-convex and the minimum fuel cost function g of the station is nonlinear and possibly discontinuous. These are the attributes that make the overall optimization problem (minimizing the fuel cost function throughout the entire system) very difficult.

4 The Fuel Cost Minimization Problem

In the previous section, we discussed in detail the mathematical model of compressor units and stations. In this section we now focus on the fuel cost minimization problem. We first state the modeling assumptions, and then present the mathematical model of the optimization problem. As we have seen in Section 3, the non-convexity of domains D and the non-convexity of function $g(v, p_s, p_d)$ (both referring to compressor stations) make the problem hard to solve. Moreover, we must also deal with pipe flow constraints (defined for every pipeline), which are also nonlinear and define a non-convex set. Since solution methodologies for general nonlinear and non-convex optimization problems are not tailored for this particular problem, what we are interested in is the special structure presented by this problem. In Section 4.2, we derive a lower bounding procedure, in which a linear supersets $\bar{D}$ of the feasible domain D is developed and a convex lower bounding function $\bar{g}$ of the minimum fuel cost function g is constructed.

4.1 Mathematical Model

We assume that the networks being considered consist of nodes, pipes, and compressor stations, only.

The objective function of the problem is the sum of the fuel costs over all the compressor stations in the network. This problem involves the following constraints:

(i) mass flow balance equation at each node;

(ii) gas flow equation through each pipe;

(iii) pressure limit constraints at each node;

(iv) operational limits in each compressor station.

The first two are also referred to as the steady-state network flow equations. We emphasize that while the mass flow balance equations are linear, the pipe flow equations are nonlinear; this has been well documented in [14]. For the medium and high pressure flows, when taking into account the fact that a change in the flow direction of the gas stream may take place in the network, the pipe flow equation takes the following form:

$$p_1^2 - p_2^2 = cu|u|^\alpha, \tag{20}$$

where p_1 and p_2 are pressures at the end nodes of the pipe, u is mass flow rate through the pipe, α is a constant ($\alpha \approx 1$), and the pipe resistance c is a positive quantity depending on the pipe physical attributes, and it is given by:

$$c = K\frac{fL}{d^5}$$

with $K = (1.3305 \times 10^5) Z S_g T$. These parameters refer to:

Z	gas compressibility factor
S_g	gas specific gravity
T	average temperature (R), assumed constant
f	frictional factor
L	length of pipe (miles)
d	inside diameter of pipe (ft)

The steady-state network flow equations can be stated in a very concise form by using incidence matrices. Let us consider a network with n nodes, l pipes, and m compressor stations. Each pipe is assigned a direction which may or may not coincide with gas flow through the pipe. Let A_l be the $n \times l$ matrix whose elements are

$$a_{ij}^{l} = \begin{cases} 1, & \text{if } j^{th} \text{ pipe comes out from } i^{th} \text{ node;} \\ -1, & \text{if } j^{th} \text{ pipe goes into } i^{th} \text{ node;} \\ 0, & \text{otherwise.} \end{cases}$$

A_l is called the node-pipe incidence matrix. Let A_m be the $n \times m$ matrix whose elements are

$$a_{ik}^{m} = \begin{cases} 1, & \text{if } i^{th} \text{ node is the discharge node of } k^{th} \text{ station,} \\ -1, & \text{if } i^{th} \text{ node is the suction node of } k^{th} \text{ station,} \\ 0, & \text{otherwise.} \end{cases}$$

A_m is thus called a node-station incidence matrix. The matrix formed by annexing A_m to the right hand side of A_l will be denoted as A, i.e., $A = (A_l \, A_m)$, which is an $n \times (l + m)$ matrix. A network example with $n = 10$ nodes, $l = 6$ pipes, and $m = 3$ stations is shown in Figure 10.

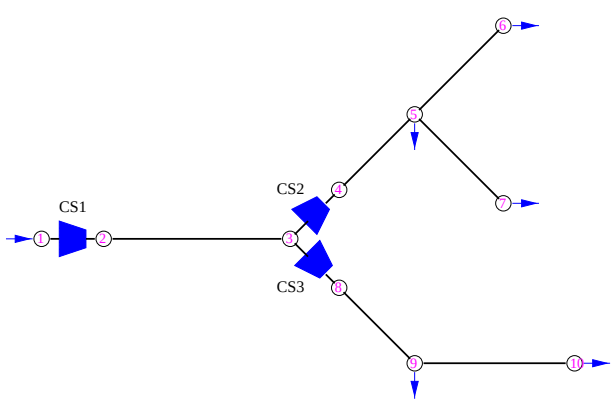

Figure 10: An example of a simple network

The nodes, pipes, and stations have been labeled separately. The matrices A_l and A_m for

this example are given by

$$A_l = \begin{pmatrix} 0 & 0 & 0 & 0 & 0 & 0 \\ 1 & 0 & 0 & 0 & 0 & 0 \\ -1 & 0 & 0 & 0 & 0 & 0 \\ 0 & 1 & 0 & 0 & 0 & 0 \\ 0 & -1 & 1 & 1 & 0 & 0 \\ 0 & 0 & -1 & 0 & 0 & 0 \\ 0 & 0 & 0 & -1 & 0 & 0 \\ 0 & 0 & 0 & 0 & 1 & 0 \\ 0 & 0 & 0 & 0 & -1 & 1 \\ 0 & 0 & 0 & 0 & 0 & -1 \end{pmatrix} \qquad A_m = \begin{pmatrix} 1 & 0 & 0 \\ -1 & 0 & 0 \\ 0 & 1 & 1 \\ 0 & -1 & 0 \\ 0 & 0 & 0 \\ 0 & 0 & 0 \\ 0 & 0 & 0 \\ 0 & 0 & -1 \\ 0 & 0 & 0 \\ 0 & 0 & 0 \end{pmatrix}$$

These matrices have some special characteristics. To name a few, each row in matrix A_l, for example, corresponds to a node, and each column corresponds to a pipe in the network. In addition, each column contains exactly two nonzero elements, one is 1 and the other -1, which correspond to the two end nodes of the pipe.

Let $\mathbf{u} = (u_1, \ldots, u_l)^T$ and $\mathbf{v} = (v_1, \ldots, v_m)^T$ be the mass flow rate through the pipes and stations, respectively, and $\mathbf{w} = (\mathbf{u}^T, \mathbf{v}^T)^T$. Let $\mathbf{p} = (p_1, \ldots, p_n)^T$ be the pressure vector, where p_i is the pressure at the i-th node, and $\mathbf{s} = (s_1, \ldots, s_n)^T$ be the source vector, where s_i is the source at the i-th node. Component s_i is positive if the node is a supply node, negative if it is a delivery node, and zero otherwise. We assume, without loss of generality, the sum of the sources to be zero,

$$\sum_{i=1}^{n} s_i = 0.$$

The network flow equations can now be stated as the follows:

$$\begin{cases} A\mathbf{w} = \mathbf{s} \\ A_l^T \mathbf{p}^2 = \phi(\mathbf{u}) \end{cases}$$

where $\mathbf{p}^2 = (p_1^2, \ldots, p_n^2)^T$ $\phi(\mathbf{u}) = (\phi_1(u_1), \ldots, \phi_l(u_l))^T$, in which $\phi_j(u_j) = c_j u_j |u_j|^\alpha$.

Now suppose the source vector $\mathbf{s}$ is given satisfying the zero sum condition, and the bounds $\mathbf{p}^L, \mathbf{p}^U$ of pressures at every node have been specified, the problem is to determine the pressure vector $\mathbf{p}$ and the flow vector $\mathbf{w}$ so that the total fuel consumption is minimized. The model is stated as follows:

$$\text{Minimize} \qquad F(\mathbf{w}, \mathbf{p}) = \sum_{k=1}^{m} g_k(v_k, p_{ks}, p_{kd}) \tag{21a}$$

$$\text{subject to} \qquad A\mathbf{w} = \mathbf{s} \tag{21b}$$

$$A_l^T \mathbf{p}^2 = \phi(\mathbf{u}) \tag{21c}$$

$$\mathbf{p} \in [\mathbf{p}^L, \mathbf{p}^U] \tag{21d}$$

$$(v_k, p_{ks}, p_{kd}) \in D_k \qquad k = 1, 2, \ldots, m \tag{21e}$$

where v_k, p_{ks}, and p_{kd} are the mass flow rate, suction pressure, and discharge pressure at the k-th station. Note that:

(i) the feasible domains D_k are non-convex;

(ii) the fuel functions g_k are nonlinear, non-convex and discontinuous;

(iii) the pipe flow equations (21c) define a non-convex set.

In general, a problem with these characteristics can be very difficult to solve. What we do in this work is to exploit the structure of this problem and derive some model relaxations that allow us to simplify the problem and to develop a lower bounding procedure. If this bound is tight enough, it can be used to evaluate the quality of feasible solutions, i.e., how close a given feasible solution is from a global optimal solution.

4.2 Model Relaxations

4.2.1 Relaxation of Compressor Domain

Recall from Section 3 that the domain D of a station is given by $\cup_{r=1}^{N} D^r$, where

$$D^r = \{(v, p_s, p_d) : (v/r, p_s, p_d) \in D^1\};$$

i.e., D^r is obtained by enlarging D^1 r times in the direction of v. Hence, by developing a superset of D^1 and then enlarging it in the v direction, a superset $\bar{D}$ of the domain D can be obtained. Such a superset $\bar{D}$ is roughly equivalent to a relaxation of the integer constraint on variable r.

As we have pointed out in Section 3, both the upper and lower surfaces bounding the domain D^1 are formed with segments of lines originated from the origin. The contour (arc ACBD, when p_s fixed) of the boundary of domain D^1 is shown in Figure 4. Hence, construction of a linear superset of D^1 can be carried out by first constructing a linear outer approximation of the contour (arc ACBD) and then connecting the linear outer contour with the origin.

For sake of simplicity and to keep the model small, we have chosen this linear approximation to consist of six hyper-planes. Our computational experience shows that this approximation is good enough. Since we have assumed in Section 3 that arc AD is convex and arc BD is concave, the linear outer approximation of arc ADB we have chosen is formed by three line segments: the first one is simply the line segment AD, the second is the horizontal line passing

through the point D, and the third is the tangent line of the upper curve at point B. The second and third lines shall intersect at some point F. The linear outer approximation of arc ACB is similar; i.e., connect A and C first, make a horizontal line pass through C, and pick the tangent line of the lower curve at point B, which intersects with the horizontal line at some point E. By our convexity assumption on the contour of D^1, these 6 line segments AD, DF, FB, BE, EC, and CA form a linear outer approximation of the contour. By connecting these 6 line segments with the origin, we get 6 planes. These planes together with another two planes, $p_s = p_s^L$ and $p_s = p_s^U$, constitute a linear superset of the domain D^1. The equations of these 6 planes, corresponding to the 6 line segments AD, DF, FB, AC, CE, and EB, respectively, take the following form:

$$p_d \quad = \quad a_i v + b_i p_s, \qquad i = 1, \ldots, 6, \tag{22}$$

where a_i, b_i, are constants which can be calculated by the values of functions G^L and G^U at points A, B, C, D, and the derivatives at point B; see equations (9)–(12) for the definition of those functions.

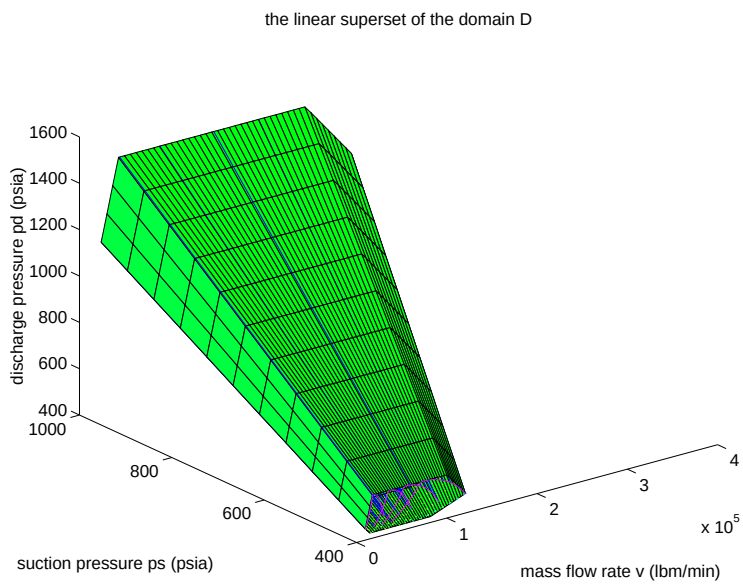

Figure 11: Superset $\bar{D}$ of the feasible domain D (station with 4 parallel units)

For the domain D of a station with N parallel identical units, the linear superset $\bar{D}$ can be easily constructed based on the linear superset of D^1. To do this, we simply move the two planes corresponding to line segments BE and BF in the direction of v until the new v value of each point is exactly N times of its original v value. The other 6 planes together with these two new planes form a linear superset $\bar{D}$ of domain D. More precisely, $\bar{D}$ consists of all the points of (v, p_s, p_d), such that

$$p_s^L \leq p_s \leq p_s^U \tag{23a}$$

and

$$
\begin{array}{lcllll}
p_d & \leq & a_1 v & + & b_1 p_s & \quad (23b) \\
p_d & \leq & & b_2 p_s & & \quad (23c) \\
p_d & \leq & a_3 v/N & + & b_3 p_s & \quad (23d) \\
p_d & \geq & a_4 v & + & b_4 p_s & \quad (23e) \\
p_d & \geq & & & b_5 p_s & \quad (23f) \\
p_d & \geq & a_6 v/N & + & b_6 p_s & \quad (23g)
\end{array}
$$

where a_i, b_i, are the same constants as in equation (22). Note that $a_2 = a_5 = 0$.

Figure 11 shows the linear superset $\bar{D}$ together with the domain D of a station with 4 units. Its profile, with p_s fixed, is given in Figure 12.

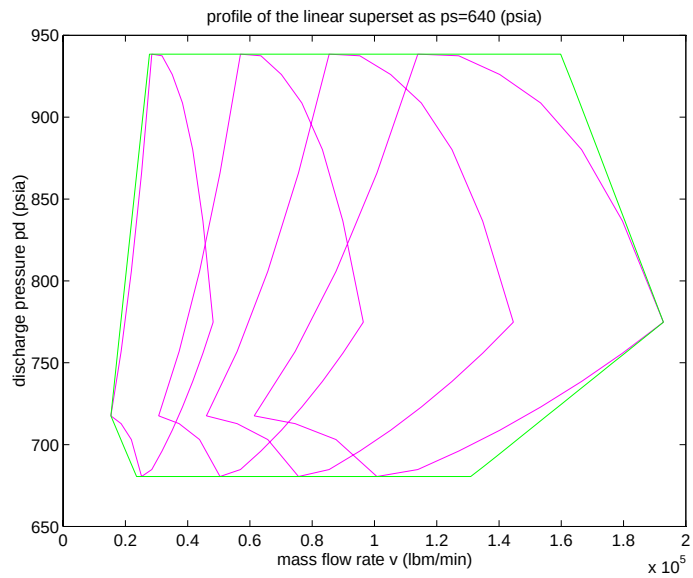

Figure 12: Profile of $\bar{D}$ and D (station with 4 parallel units)

In the next section, we will investigate the properties of the minimum fuel cost function g of a station and describe how to develop a convex lower bounding function $\bar{g}$ for g.

4.2.2 Relaxation of Cost Function

Recall from Section 3 that the minimum fuel cost function $g(v, p_s, p_d)$ of the station is defined as

$$g(v, p_s, p_d) = \min_{r \in \mathcal{R}} \{ r g^{\text{unit}}(v/r, p_s, p_d), \} \tag{24}$$

where

$$
\begin{aligned}
\mathcal{R} &= \{ r : r \text{ is integer }, \ 1 \leq r \leq N, \ (v, p_s, p_d) \in D^r \} \\
D^r &= \left\{ (v, p_s, p_d) : \ p_s^L \leq p_s \leq p_s^U, \ V^L \leq \frac{v}{r p_s} \leq V^U, \ G^L(\frac{v}{r p_s}) \leq \frac{p_d}{p_s} \leq G^L(\frac{v}{r p_s}) \right\}.
\end{aligned}
$$

The idea we introduce to get a convex lower bound for function g is quite general. First, we find a set of linear lower bounds of $\bar{g}$, say,

$$l^i(v, p_s, p_d) = a^i v + b^i p_s + c^i p_d + d^i \quad \leq \quad g(v, p_s, p_d), \quad i \in I,$$

where I is an index set. Let

$$l(v, p_s, p_d) \quad = \quad \max_{i \in I} \left\{ l^i(v, p_s, p_d) \right\},$$

then we have

$$l(v, p_s, p_d) \quad \leq \quad g(v, p_s, p_d).$$

Classical theory of linear programming [5] shows that l is convex. Therefore l is a piece-wise linear convex lower bound of g. Figure 13 illustrates this idea in one dimension, in which an arbitrary function $z = f(x)$ of one variable $x \in [a, b]$ is plotted. To generate a set of linear lower bounds of function $z = f(x)$ on $[a, b]$, the procedure is divided into the following steps:

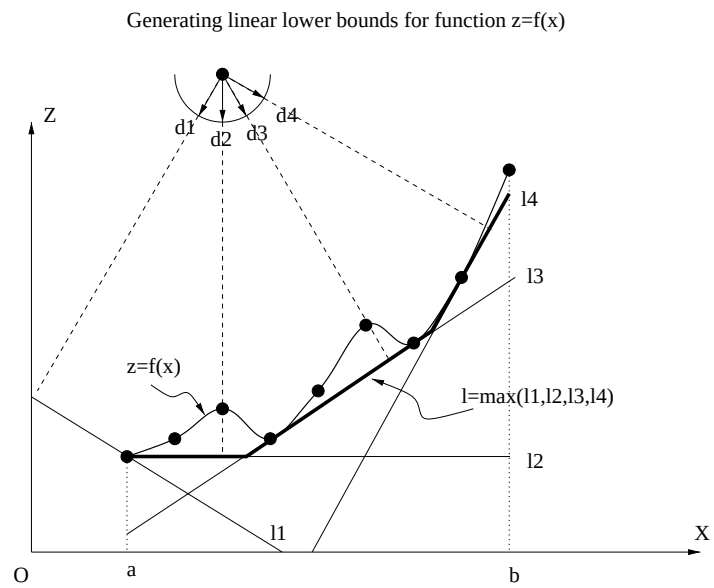

Figure 13: Generating linear lower bounds for an arbitrary function

Step 1: Grid Generation. By partitioning the interval $[a, b]$, we generate a set of grid points on the curve of the function $z = f(x)$.

Step 2: Direction Selection. The second step is selecting a few directions (four directions d_1, d_2, d_3, and d_4 have been selected in Figure 13).

Step 3: Along each direction, we minimize the function $z = f(x)$. Since it is not always guaranteed that the global minimization can be found for an arbitrary function, instead

of doing that we find the grid point at which the function $z = f(x)$ achieves its minimum along this direction among all the grid points generated in step 1.

Step 4: The line passing through the found grid point with the direction as its normal is thus a linear (pseudo) lower bound (not exact lower bound because the minimization is taken only over the grid points) of function $z = f(x)$ on $[a, b]$. Four such linear bounds l_1, l_2, l_3, and l_4 have been plotted in Figure 13, and their maximum l is a convex (pseudo) lower bound of function $z = f(x)$ on $[a, b]$.

A few remarks on the above procedure:

1. In the second step, the direction $d_i = (x_i, z_i)$ selected must have $z_i < 0$. Otherwise, the minimization in step 3 does not make any sense because we are generating a lower bound.

2. Without any more information (particularly about convexity) of the function, there is no way to generate absolute but also good lower bounds. The above procedure will deliver a piece-wise linear lower bound for any given function. Theoretically, as the number of the grids generated in step 1 goes to infinity, this procedure could produce the best convex lower bound, i.e., the convex envelope of the given function. The fact is, even with a reasonable number of grid points and directions, the above procedure may also produce a quite satisfactory result.

3. The above procedure is especially practical for functions of only a few variables. In our case the cost function is defined over a three-dimensional space (mass flow, suction pressure, and discharge pressure), so applying the proposed procedure is not too expensive.

5 Numerical Evaluation

In this section, we provide empirical evaluation of the proposed lower bounding procedure. To do this, we construct three network examples based on network topologies commonly encountered in practice. The data for the compressor stations is taken from some real-world instances. We must note that at present, no data library of instances for this type of problems exists. So we hope that this set of problem instances could become the starting point for building such a data base, that would allow for testing other approaches and benchmarking.

In our numerical calculations, the following data are used through all the examples.

Gas: The gas is a mixture with a volumetric composition of 14% ethane, 85% methane, and 1% nitrogen. The values of its parameters are isentropic exponent $k = 1.287$, compressibility factor $Z = 0.95$, and gas constant $R = 85.2$(lbf-ft)/(lbm-°R), and specific gravity $S_g = 0.6248$.

Station: Stations consist of N centrifugal compressor units. All the units used in examples are identical. The fitted coefficients of equations (1) and (2) are given by $A_H = 0.6824 \times 10^{-3}$, $B_H = -0.9002 \times 10^{-3}$, $C_H = 0.5689 \times 10^{-3}$, $D_H = -0.1247 \times 10^{-3}$, $A_E = 134.8055$, $B_E = -148.5468$, $C_E = 125.1013$, $D_E = -32.0965$. The compressor limits for speed (rpm) and volumetric flow rate (ft^3/min) as defined in equations (3) and (7), respectively, are given by $S_{\min} = 5000$, $S_{\max} = 9400$, $Q^L = 7000$, and $Q^U = 22000$. The feasible domain D of the stations is defined by (8), (17), and (18). The superset domain $\bar{D}$ of D is defined by (23a)–(23g), where $a = \{0.0185, 0, -0.0328, -0.0047, 0, 0.0096\}$ and $b = \{0.6778, 1.4729, 3.6853, 1.2332, 1.0620, 0.4921\}$. The fuel cost function $g^{\text{unit}}(v, p_s, p_d)$ for a compressor unit used is the approximation $g_6(v, p_s, p_d)$ given by (16f), where $A_6 = 0.0266$, $B_6 = 38.1969$, $C_6 = -3.4865$, $D_6 = 2.3791$, $E_6 = 439.7503$, $F_6 = -460.6632$. The minimum fuel cost function $g(v, p_s, p_d)$ for a compressor station is defined by (24).

Pipe Flow Equation: For the pipe flow constraint (20) we assume the average temperature $T = 459.67 + 60(^\circ R)$, which gives $K = 4.1040 \times 10^7$.

For the objective function relaxation we used 27 directions, defined by $(d_v, d_{p_s}, d_{p_d}, -1)$, where $d_v, d_{p_s}, d_{p_d} \in \{-1, 0, 1\}$, are the components in the v, p_d, and p_d directions, respectively. The four (-1) components correspond to the direction in the field function $g(v, p_s, p_d)$.

With the relaxations on the minimum fuel cost function $g(v, p_s, p_d)$ and the feasible domain D, we consider four different problems related to the original problem (21a)-(21e), namely:

P1: the original problem itself;

P2: the original problem with relaxation of the function $g(v, p_s, p_d)$ only;

P3: the original problem with relaxation of the domain D only;

P4: the original problem with relaxations both of the domain D and the function $g(v, p_s, p_d)$.

It is clear that an optimal solution to P2, P3, or P4 renders a lower bound for the original problem P1. The motivation for defining these four problems is to assess the performance of the lower bound function and domain D relaxations, both jointly and individually. To achieve this, we use three network configurations. The first two are relatively small, so we were able to solve all P1–P4 for each example by exhaustive enumeration over a finite grid. The third example is a larger and more complex network, so optimal solutions by exhaustive enumeration is very impractical. We resorted to finding a solution to a relaxation of P4, which still preserves the lower bound property.

5.1 Example 1

The first example is a 6-node, 3-pipe, 2-compressor network. The arcs form a straight path (called a gun-barrel network in the pipeline world) as shown in Figure 14. There is a supply node (node 1) and a delivery node (node 6) with source values $s_1 = +600$ and $s_6 = -600$ (MMSCFD), respectively. For all other nodes $s_i = 0$. The pressure ranges for each node is $[600, 800]$ (psia). The set of pipes is given by $\{(1,2),(3,4),(5,6)\}$. For each pipe, length=50 (miles), inside diameter = 3 (ft), and friction factor = 0.0085. The set of compressors is given by $\{(2,3),(4,5)\}$. Each compressor station has 5 centrifugal units in parallel.

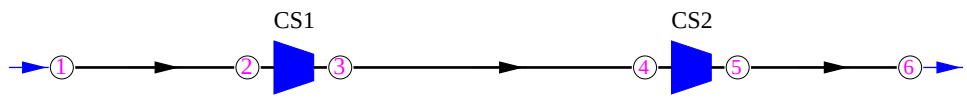

Figure 14: Example 1 network

The flow rates through all pipes can be determined before hand, so only the pressure variables need to be found. Since the problem size is relatively small, problems P1, P2, P3, and P4 can be solved by exhaustive search. We built a grid for the pressures using a discretization size of $\Delta p = 3$ (psia), and solved problems P1–P4 using Matlab [4]. The results are presented in Table 2.

Problem	Solution ($\times 10^6$)
P1	2.140172
P2	2.112003
P3	1.824072
P4	1.732357

Table 2: Example 1 results

As can be seen, the relative gap between P1 and P4 is 23.5%. We also observe that that the gap difference between P1 and P2 is smaller than the gap difference between P1 and P3. This implies than the relaxation of the objective function does a better job than the relaxation of the compressor domain. Similar results are observed when we compare the gap difference between P3 and P4 to the gap difference between P2 and P4.

5.2 Example 2

The second example is a simple tree network with 10 nodes, 6 pipes and 3 compressor stations, as depicted in Figure 15. The network includes one supply node (node 1) $s_1 = +800$ and five delivery nodes (nodes 5, 6, 7, 9 10), with $s_5 = s_9 = -100$, $s_6 = s_7 = -150$, and $s_{10} = -300$. The

pressure lower limits are given by $p_1^L = p_2^L = 600$, $p_3^L = p_5^L = p_6^L = p_7^L = p_9^L = 450$, $p_4^L = 500$, $p_5^L = p_{10}^L = 400$ and $p_8^L = 550$. The pressure upper limit is $p_1^U = 700$ and $p_i^U = 800$, for all $i > 1$. The set of pipes is $\{(2,3),(4,5),(5,6),(5,7),(8,9),(9,10)\}$ with length $= 50$, inside diameter $= 3$, and friction factor $= 0.0085$, for all pipes. The compressor stations $\{(1,2),(3,4),(3,8)\}$ all have five centrifugal units operating in parallel.

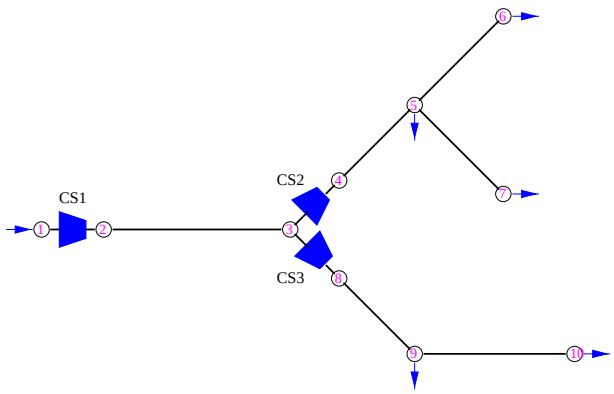

Figure 15: Example 2 network

As in the previous example, the flow rates through all pipes and stations can be determined during preprocessing, thus leaving us with the pressure variables only. We again set up a Matlab program that would solve problems P1–P4 by an exhaustive method over a grid of size $\Delta p = 3$. Table 3 displays the results.

Problem	Solution ($\times 10^6$)
P1	2.699550
P2	2.515808
P3	2.580367
P4	2.350785

Table 3: Example 2 results

As we can see, the relative gap between P1 and P4 is 14.8%. However, note that this time the gap difference between P3 and P1 is smaller than the gap difference between P1 and P2, which means that the relaxation of the compressor station domain does better than the relaxation of the objective function. This is contrary to what we had observed in Example 1. One explanation for this is that, for both problems we are using the same number of underestimating planes (nine) for the objective function relaxation, but for Example 1, the pressure ranges are much narrower, which makes the function relaxation have a better fit. Note that the compressor domain relaxation is not affected by the change in the pressure ranges.

5.3 Example 3

The third example (depicted in Figure 16) is a more complex network. There are 48 nodes, 43 pipes, and 8 stations. Moreover, it contains several loops so the flow rates cannot be determined before hand.

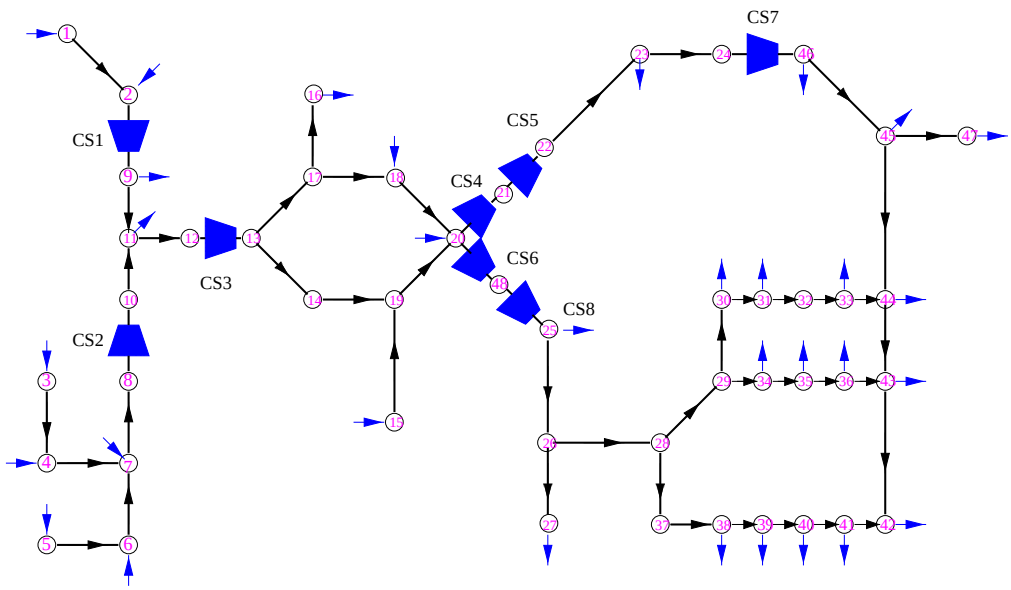

Figure 16: Example 3 network

i	s_i	i	s_i	i	s_i	i	s_i
1	+600	13	0	25	-550	37	0
2	0	14	0	26	0	38	-30
3	+200	15	+100	27	-50	39	-30
4	+200	16	-50	28	0	40	-30
5	+200	17	0	29	0	41	-30
6	+200	18	100	30	-30	42	-40
7	+200	19	0	31	-30	43	-40
8	0	20	+450	32	0	44	-40
9	-400	21	0	33	-30	45	-100
10	0	22	0	34	-30	46	-200
11	-100	23	-200	35	-30	47	-180
12	0	24	0	36	-30	48	0

Table 4: Node source values for Example 3

The following three tables list the sources at all the nodes, the pipe configuration, and the station configuration. The pressure limits at all the nodes are [50,1500], except for nodes 1 ([900,1300]) and 3 ([990, 1150]). The source values are given in Table 4. The pipe data, nodes, length (L), inside diameter (d), and friction factor (f), are shown in Table 5. The compressor

station set is $\{(2,9),(8,10),(12,13),(20,21),(21,22),(20,48),(24,46),(48,25)\}$. Each station has five centrifugal units running in parallel.

Pipe	L	d	f	Pipe	L	d	f
(1,2)	10.1015	1.5	0.0108	(30,31)	5.0507	1.0	0.0130
(3,4)	4.5175	1.5	0.0108	(31,32)	4.5175	1.0	0.0130
(4,7)	5.1508	1.5	0.0108	(32,33)	4.5175	1.0	0.0130
(5,6)	5.1508	1.0	0.0130	(33,44)	4.5175	1.0	0.0130
(6,7)	5.1508	1.5	0.0108	(29,34)	5.0507	1.0	0.0130
(7,8)	5.1508	2.0	0.0090	(34,35)	4.5175	1.0	0.0130
(9,11)	10.1015	1.5	0.0108	(35,36)	4.5175	1.0	0.0130
(10,11)	5.1508	2.0	0.0090	(36,43)	4.5175	1.0	0.0130
(11,12)	10.1015	3.0	0.0085	(28,37)	5.0507	1.0	0.0130
(13,14)	10.1015	1.5	0.0108	(37,38)	5.0507	1.0	0.0130
(14,19)	10.1015	1.5	0.0108	(38,39)	5.0507	1.0	0.0130
(15,19)	10.1015	1.5	0.0108	(39,40)	5.0507	1.0	0.0130
(19,20)	10.1015	1.5	0.0108	(40,41)	5.0507	1.0	0.0130
(13,17)	10.1015	2.0	0.0095	(41,42)	5.0507	1.0	0.0130
(17,16)	10.1015	1.5	0.0108	(43,42)	4.5175	1.0	0.0130
(17,18)	10.1015	2.0	0.0095	(44,43)	4.5175	1.0	0.0130
(18,20)	10.1015	2.0	0.0095	(45,44)	8.3299	1.5	0.0108
(25,26)	10.1015	1.5	0.0108	(45,47)	5.7143	2.0	0.0090
(26,27)	7.1429	1.5	0.0108	(46,45)	11.5175	2.0	0.0090
(26,28)	10.1015	1.5	0.0108	(22,23)	11.5175	2.0	0.0090
(28,29)	5.0507	1.0	0.0130	(23,24)	11.4286	2.0	0.0090
(29,30)	4.5175	1.0	0.0130				

Table 5: Pipe data for Example 3

For this example, the presence of loops implies that flow rates are not uniquely determined and thus form part of the problem decision variables, along with the pressure variables. In addition, the size of this instance leaves the possibility of computing exact solutions by exhaustive enumeration out of question. Since optimal solutions for problems P1–P4 were not possible to obtain, we found some upper and lower bounds for some of these problems, as shown in Table 6. An upper bound is computed by finding a feasible solution for the corresponding problem. For problem P4, we computed a lower bound by using a Lagrangian relaxation technique where the pipe leg constraints are relaxed (see Ríos-Mercado [11] for details). This relaxation was implemented in GAMS [1], an algebraic modeling software package with interfaces to several optimization libraries.

As we can see, the relative gap between the two bounds (upper bound for P1 and lower bound for P4) is very large (about five times larger). In order to explain this big difference between the bounds, we first observe that the Lagrangian relaxation approach for P4 is doing a very good job at bounding P4 providing a relative gap of less that 0.5% with respect to its

Problem	Lower bound ($\times 10^6$)	Upper bound ($\times 10^6$)
P1	–	25.69718
P2	–	–
P3	–	14.98100
P4	4.53535	4.55604

Table 6: Example 3 results

upper bound. Now, assuming that the upper bound for P3 is relatively close to the optimal value, the solution to P3 would be about three times as big as the solution to P4. This suggests the convex function relaxation $\bar{g}$ might not be a good approximation of the objective function g. To investigate this further, we display in Table 7, different objective function values achieved at the individual compressor stations. In the first column, we show the minimum value of g within each individual compressor station domain ($g_{\min}$). In the second column, we show the value the convex under-estimator function $\bar{g}$ takes in a given compressor domain, after solving the P4 Lagrangian relaxation. The third column, shows the value of objective function g, after a feasible solution for P3 has been computed.

Station	$g_{\min}$	$\bar{g}$	g
(2,9)	7.05	7.06	11.71
(8,10)	11.18	11.19	16.13
(12,13)	12.44	12.45	72.50
(20,21)	3.18	3.37	10.13
(21,22)	3.18	3.37	11.36
(20,48)	2.47	2.76	9.79
(24,46)	2.47	2.61	6.99
(48,25)	2.46	2.76	11.21

Table 7: Objective function values among stations

We first observe that the values in the first two columns are very similar. This implies that the convex under-estimator $\bar{g}$ is indeed doing a good job of approximating the true g within each individual compressor station. On the other hand, we also observe that the difference in the gaps between P3 and P4 is due to the difference between the values of columns 2 and 3 in this table. This stems from the fact that an individually good solution for a compressor station is not necessarily a good solution for the overall problem, when the contributions of all the compressors are taken into account. The non-convexity of the set defined by the pipeline constraints obviously play a very important practical role here.

6 Conclusions

We have presented a study of the mathematical structure of compressor stations in natural gas transmission networks. We have analyzed several important properties of both the set of feasible operating conditions and the associated cost function.

The fuel cost minimization model has been presented. We have highlighted why this problem is difficult to solve (namely the nonlinearity, non-convexity, and discontinuity in the objective function, and the non-convexity of the feasible set). We have proposed and derived two model relaxations that allowed us to develop a lower bounding scheme. One relaxation consisted of developing linear supersets $\bar{D}$ of the feasible domains D. The other is the derivation of piecewise linear under-estimator functions $\bar{g}$ of the minimum fuel cost functions g for the compressor stations.

The proposed procedures have been tested on three test examples made from real-world data. For the first two examples, we have found lower bounds with relative gaps of 23% and 15%, respectively. These gaps were with respect to optimal solutions of the problems. The results for the small problems show that the proposed relaxations are in fact good. For the third example, the relative gap was very wide. We observed that the convex under-estimator function was indeed a very good approximation to the function within each of the compressor stations. However, when optimizing over the complete domain, the overall bound was not good due mainly to the non-convexity of the set of feasible solutions and to the presence of multiple local optima in the fuel cost function g.

As is well known, techniques for finding global optimal solutions to non-convex problems, such as branch and bound, rely heavily on the capacity of generating good lower bounds. Further research in this area is needed for handling larger instances more effectively. A transient, or time dependent, model is another important problem that to date has not been adequately addressed from the optimization perspective.

We should also mention the need for having a library of data sets, that would allow more uniform algorithm testing and benchmarking among researchers and practitioners working in this area.

7 Acknowledgments

This research has been funded by the NSF (grant No. DMI–9622106) and by the Texas Higher Education Coordinating Board under its Advanced Research Program (grant No. 999903–122). Our work also benefit from helpful discussions with Peter Percell, Richard Carter, Don Schroeder, and Todd Dupont.

References

[1] A. Brooke, D. Kendrick, and A. Meeraus. *GAMS: A User's Guide, Release 2.25.* The Scientific Press, San Francisco, 1992.

[2] R. G. Carter. Pipeline optimization: Dynamic programming after 30 years. In *Proceedings of the 30th PSIG Annual Meeting*, Denver, October 1998.

[3] H. S. Lall and P. B. Percell. A dynamic programming based gas pipeline optimizer. In A. Bensoussan and J. L. Lions, editors, *Analysis and Optimization of Systems*, volume 144 of *Lecture Notes in Control and Information Sciences*, pages 123–132, Berlin, 1990. Springer-Verlag.

[4] The MathWorks, Inc., Natick, Massachusetts. *MATLAB User's Guide*, 1992.

[5] K. G. Murty. *Linear Programming.* Wiley, New York, 1983.

[6] A. J. Osiadacz. *Simulation and Analysis of Gas Networks.* Gulf Publishing Company, Houston, 1987.

[7] A. J. Osiadacz. Dynamic optimization of high pressure gas networks using hierarchical systems theory. In *Proceedings of the 26th PSIG Annual Meeting*, San Diego, October 1994.

[8] A. J. Osiadacz and M. Górecki. Optimization of pipe sizes for distribution gas network design. In *Proceedings of the 27th PSIG Annual Meeting*, Albuquerque, October 1995.

[9] A. J. Osiadacz and S. Swierczewski. Optimal control of gas transportation systems. In *Proceedings of the 3rd IEEE Conference on Control Applications*, pages 795–796, August 1994.

[10] P. B. Percell and M. J. Ryan. Steady-state optimization of gas pipeline network operation. In *Proceedings of the 19th PSIG Annual Meeting*, Tulsa, October 1987.

[11] R. Z. Ríos-Mercado. Lagrangian relaxations for minimum cost gas transmission networks. Manuscript, Department of Industrial Engineering, Texas A&M University, May 1998.

[12] D. W. Schroeder. Hydraulic analysis in the natural gas industry. In J. J.-W. Chen and A. Mital, editors, *Advances in Industrial Engineering Applications and Practice I*, pages 960–965, Cincinnati, Ohio, 1996. International Journal of Industrial Engineering.

[13] P. J. Wong and R. E. Larson. Optimization of natural-gas pipeline systems via dynamic programming. *IEEE Transactions on Automatic Control*, AC–13(5):475–481, 1968.

[14] S. Wu. *Steady-State Simulation and Fuel Cost Minimization of Gas Pipeline Networks.* PhD thesis, University of Houston, Houston, August 1998.

[15] S. Wu, E. A. Boyd, and L. R. Scott. Minimizing fuel consumption at gas compressor stations. In J. J.-W. Chen and A. Mital, editors, *Advances in Industrial Engineering Applications and Practice I*, pages 972–977, Cincinnati, Ohio, 1996. International Journal of Industrial Engineering.